J. CHEM. SOC. FARADAY TRANS., 1994, 90(19), 2953–2960

Investigation of the Structure of the Columnar Liquid-crystalline Phase of Copper(II) Carboxylates

An FTIR Spectroscopic Study

Maria F. Ramos Moita and Maria Leonor T. S. Duarte
Departamento de Química, Universidade de Lisboa, P-1700 Lisboa, Portugal
Rui Fausto*
Departamento de Química, Universidade de Coimbra, P-3049 Coimbra, Portugal

The FTIR spectra of a series of anhydrous copper(II) carboxylates of general formula $Cu_2[CH_3(CH_2)_nCO_2]_4$ (n = 4–8, 10, 12, 14 and 16) have been studied as a function of temperature. The spectra show notable changes associated with the phase transition from the crystalline to the columnar liquid-crystalline phase which indicate that the coordination of the carboxylate groups to the bimetallic centre changes from bridging bidentate to chelating bidentate. The observed change in the type of coordination is induced by the conformational disordering to the carbon chains and does not affect strongly the chemical environment around the copper atoms (in particular the Cu—Cu and Cu—O distances), in agreement with previous Cu-Kα EXAFS spectroscopic results.

Carboxylate complexes of transition metals [in particular those of copper(II)] have been the subject of many studies.[1–4] Indeed, besides their practical importance in industry,[5,6] these compounds present very interesting physicochemical properties[6,7] which also make them a challenge to fundamental investigation.

The crystal structure of some copper(II) carboxylates [for example, copper(II) butyrate, octanoate and decanoate] at room temperature has been determined by X-ray crystallography[8–10] and it was shown that these compounds exhibit a tetrakis(carboxylate)dimetal (bridging bidentate) coordination in the crystalline lamellar phase (Fig. 1), in which planes of polar copper carboxylate groups are separated by a double layer of aliphatic chains.[11,12] It was also found that two of the carbon chains adopt an all-*trans* structure, while the remaining two present a *gauche* conformation near the metal centre, in order to facilitate the crystal packing.[8–13]

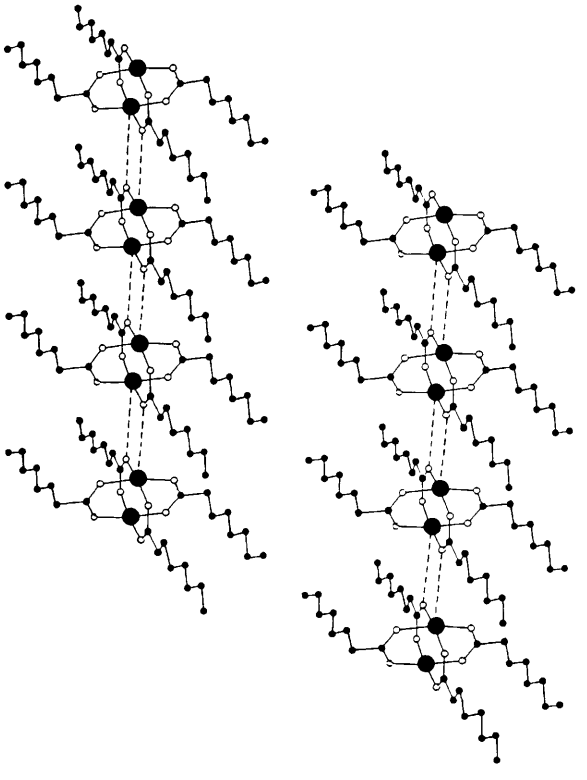

Fig. 1 Schematic representation of the lamellar phase (crystal) of copper carboxylates

Upon heating, the copper(II) carboxylates that have a carbon chain with at least five carbon atoms exhibit liquid-crystalline mesophases.[7,11,12] Above *ca.* 120 °C, a columnar liquid-crystalline phase is formed, consisting of columns of carboxylate polar groups surrounded by disordered aliphatic chains forming a two-dimensional hexagonal lattice.[7,11,12] From Cu-Kα EXAFS spectroscopic studies,[3,14] it was found that the local environment of the copper atoms in this mesophase is similar to that found in the crystalline phase. In particular, the number of oxygen atoms around each copper atom is the same and the Cu—O bond lengths do not change appreciably. In addition, only a very slight increase in the Cu—Cu bond length seems to occur at the phase transition. On the other hand, magnetic susceptibility measurements[14,15] indicated that a sharp drop of the susceptibility occurs near the solid → mesophase transition-temperature. This feature was assigned to a structural modification of the polar core of the molecules at the phase transition which affects mainly the bond angles near the bimetallic centre.[14]

Though some important features of the structure of this mesophase have already been established,[3,11,12,14–16] its precise characterization at a molecular level had not yet been established. In particular, as referred to above, the rearrangement associated with the solid → mesophase transition had not yet been clearly elucidated. In the present study, FTIR spectroscopy is used to monitor the solid → mesophase transition in a series of anhydrous copper(II) carboxylates {$Cu_2[CH_3(CH_2)_nCOO]_4$; n = 4–8, 10, 12, 14 and 16, abreviated CuC_{n+2}} and to shed light on the associated structural changes.

Experimental

Anhydrous copper(II) carboxylates were synthesised by two slightly different methods, depending on the size of their carbon chain. The smaller compounds (CuC_6–CuC_9) were obtained from equal volumes of 0.5 mol dm^{-3} hot aqueous solutions of the corresponding carboxylic acid and copper(II) acetate. The two solutions were mixed under vigorous stirring conditions and, after completion of the reaction, the

copper carboxylate precipitate was washed with Millipore water and ethanol, and then dried by gentle heating (60 °C) under vacuum for 48 h. The synthesis and purification procedures used for preparation of the longer-chain carboxylates (CuC_{10}–CuC_{18}) were similar to those used for the preparation of the shorter-chain complexes, but because of the reduced solubility of the corresponding carboxylic acids in water, these were initially dissolved in ethanol. All of the reagents used were commercial grade purity. The copper complexes have all been characterized by elemental analysis (C, H) and the results are reported in Table 1. In addition, X-ray diffraction studies of powder samples at room temperature, as well as temperature-variable polarized-light optical microscopy and differential scanning calorimetry studies were carried out on all compounds either to evaluate their degree of crystallinity or to confirm their purity using the crystal–mesophase transition-temperatures previously reported[11,12] (see Table 1).

IR spectra of the copper complexes in the crystalline state as KBr pellets were obtained on a Perkin Elmer 1760 FTIR spectrometer, equipped with a KBr beam splitter and a DTGS detector with CsI windows, over the wavenumber range 4000–400 cm^{-1}, with 32 scans and a spectral resolution of 2 cm^{-1}, at room temperature. IR spectra at elevated temperatures (mesophases) were recorded on a Nicolet FTIR 800 system (32 scans; spectral resolution 2 cm^{-1}), equipped for the 4000–400 cm^{-1} region with a germanium on CsI beam splitter and a DTGS detector with CsI windows, using a specially designed transmittance high-temperature cell with KBr windows, linked to a VENTACON (Winchester) model CAL 9000 temperature controller.

Molecular modelling was performed using the MOLECULAR EDITOR program,[17] running on a Macintosh computer.

Results and Discussion

The IR spectra of all studied compounds, although showing marked differences when going from the crystalline to the liquid-crystalline columnar phase, show very similar profiles within each phase. Thus, in Fig. 2 only the spectra of the compounds CuC_6, CuC_{12} and CuC_{18} are presented. A general assignment of the main features observed in the spectra of these compounds, as well as in those of the remaining molecules studied, is presented in Table 2. Note that the vibrational assignments are in consonance with those we have reported previously for a typical long-chain copper(II) carboxylate in the crystalline phase[18] and are supported by detailed analyses of the IR spectra of a series of copper(II) short-chain carboxylates (acetate, propionate, butyrate[18,19]).

The main spectral differences observed in going from the crystalline phase to the columnar mesophase occur in two spectral regions (1600–1400 and 800–600 cm^{-1}) and the discussion that follows centres on the analysis of these regions.

1600–1400 cm^{-1} Region

It is well known that both ν_{COO} stretching modes (symmetric and antisymmetric) give rise to bands in this region. In the crystal, the antisymmetric mode gives rise to the very intense IR band near 1585 cm^{-1} (sometimes exhibiting complex structure due to crystal-field splitting effects), while the symmetric vibration originates the considerably less intense band at *ca.* 1425 cm^{-1} (*ca.* 1416 cm^{-1}, in the smaller compounds) which usually partially overlaps the bands due to the polymethylene δ_{CH_2} scissoring vibrations.[18–20] Several authors have proposed[20–24] that the relative position of these two bands ($\Delta\nu_{COO} = \nu_{COO,as} - \nu_{COO,s}$) can be used to shed light on the type of carboxylate-to-metal complexation structure present in a given metal carboxylate. In particular, it has been established that if, as in the studied molecules, both $\nu_{COO,as}$ and $\nu_{COO,s}$ frequencies are shifted in the same direction with respect to those observed for the free carboxylate ion (*ca.* 1565 and 1410 cm^{-1},[19,25] respectively), the coordination is either bridging bidentate (structure **I**, Fig. 3) or chelating bidentate (structure **II**, Fig. 3).[20] This may be easily understood as it is expected that in these two types of coordination the bond orders of both CO bonds would change by nearly the same amount with respect to those of the free ion (indeed, this is only strictly true for symmetric coordinating structures; non-symmetric coordination may lead to different, though comparable, shifts). In addition, it was also found that a $\Delta\nu_{COO}$ of *ca.* 150–170 cm^{-1} correlates with a bridging bidentate mode of coordination, while chelating bidentate structures usually give rise to $\Delta\nu_{COO} \approx 100$ cm^{-1}.[19,24] Note that all the studied copper(II) carboxylates, in the crystalline state, have $\Delta\nu_{COO} \approx 160$–170 cm^{-1} (Table 3), in agreement with their known bridging bidentate coordination structure in this phase.

The spectra of the columnar mesophases differ considerably in this spectral region from those corresponding to the crystalline phase (Fig. 4). In particular, (i) a new band is observed at *ca.* 1540 cm^{-1} (in general showing a shoulder at *ca.* 1530 cm^{-1}), (ii) the band at *ca.* 1585 cm^{-1} ($\nu_{COO,as}$ in the crystal) is considerably reduced in intensity, (iii) the band ascribed to the $\nu_{COO,s}$ mode splits, giving rise to a pair of overlapped bands at *ca.* 1425 and 1417 cm^{-1} and (iv) the bands observed in the 1450–1400 cm^{-1} region due to the δ_{CH_2} scissoring and δ_{CH_3} antisymmetric bending modes are considerably broadened.

Table 1 Elemental analysis[a] (C, H) and crystal → mesophase transition temperatures of the copper carboxylates

compound	C(%)			H(%)			transition temperature[b]/°C
	calc.	exp.	exp.	calc.	exp.	exp.	
CuC_6	49.05	48.58	48.81	7.49	7.56	7.57	95
CuC_7	52.24	51.89	51.86	8.08	8.19	8.21	92
CuC_8	54.91	54.89	54.84	8.57	8.73	8.78	85
CuC_9	57.19	56.84	56.74	8.99	9.17	9.16	99
CuC_{10}	59.16	58.00	57.90	9.43	9.38	9.41	105
CuC_{12}	62.37	60.43	60.36	10.03	10.00	9.99	107
CuC_{14}	64.89	62.92	63.05	10.50	10.48	10.51	116
CuC_{16}	66.92	63.73	63.75	10.88	10.66	10.67	116
CuC_{18}	68.58	65.45	65.46	11.10	10.98	10.97	116

[a] Two sets of experimental data are presented. [b] Results obtained by differential scanning calorimetry and corresponding to the onset of the phase transition upon heating.

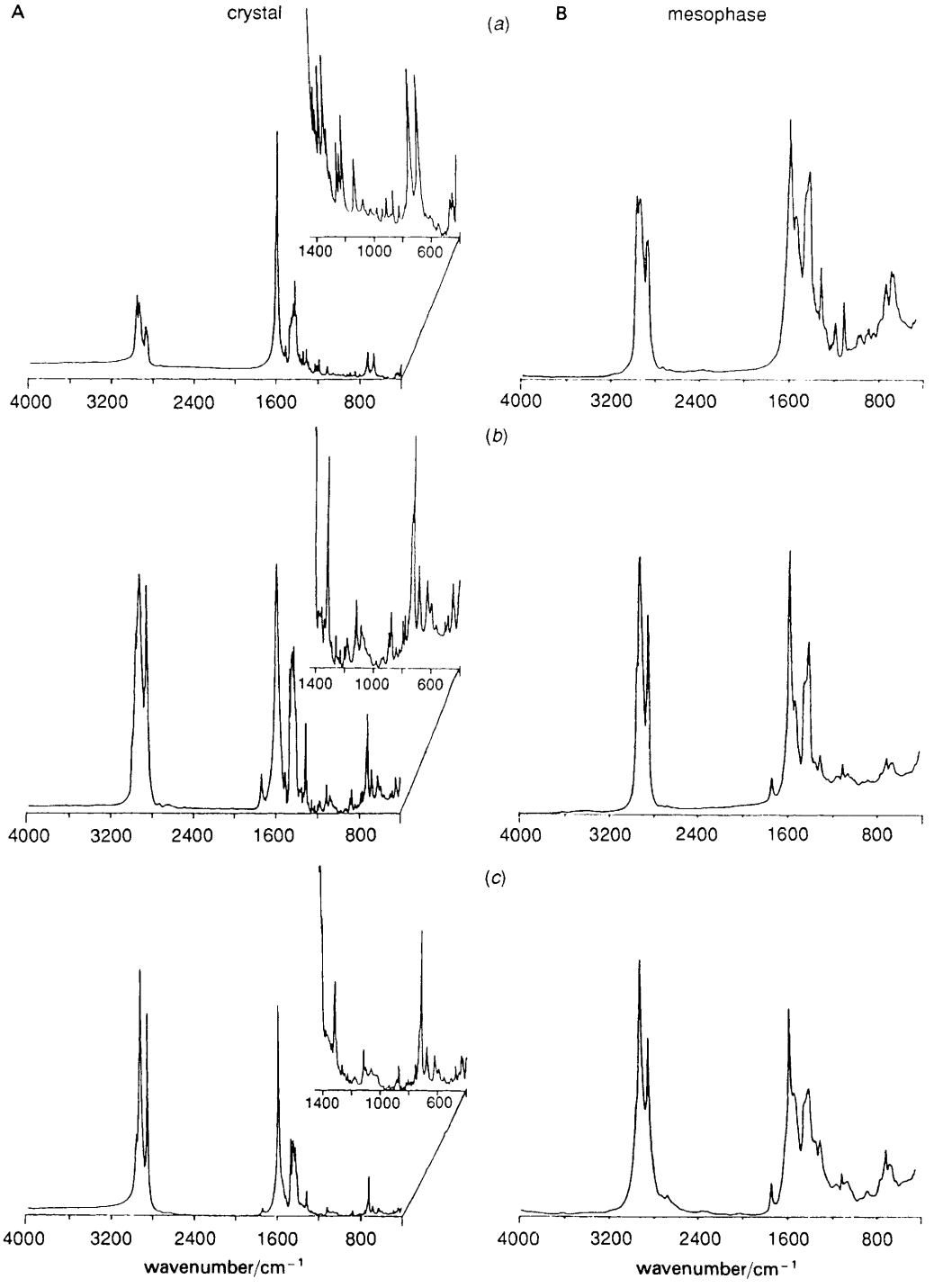

Fig. 2 FTIR spectra of A, crystalline (room temperature) and B, columnar liquid-crystalline ($T \approx 150\,^{\circ}C$) phases of copper(II) carboxylates: (*a*) CuC_6, (*b*) CuC_{12} and (*c*) CuC_{18}

The observed broadening of the bands due to the CH bending modes can be easily attributed to the increased number of methylene carbon chain *gauche* arrangements and, thus, is a direct consequence of the increased conformational disorder of the system in the mesophase. Furthermore, this interpretation is reinforced by considering the observed systematic increase in the peak intensity ratio I_{2920}/I_{2850} ($\nu_{CH_2,as}$ stretching/$\nu_{CH_2,s}$ stretching) in going from the crystal to the mesophase in the various molecules studied (Table 3). Indeed, it has been shown by several authors that the above-mentioned intensity ratio is a good measure of the conformational disorder and lateral packing of a polymethylene chain,[26–28] increasing with the number of *gauche* arrangements. Thus, it can be concluded that the onset of the conformational disordering of the carbon chains plays a decisive role in determining, at a molecular level, the formation of the mesophases in the studied compounds. Furthermore, this

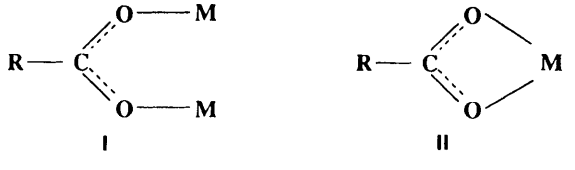

Fig. 3 Schematic representation of the carboxylate–metal bridging (**I**) and chelating (**II**) types of coordination

Table 2 Vibrational assignments[a]

	wavenumber/cm^{-1}							
	CuC_6		CuC_7		CuC_8		CuC_9	
assignment	crystal	mesophase	crystal	mesophase	crystal	mesophase	crystal	mesophase
$\nu_{CH_3,\,as}$	2964	2957	2968	2957	2963	2957	2968	2957
$\nu_{CH_3,\,as}$	2954	2957	2954	2957	2953	2957	2956	2957
$\nu_{CH_3,\,s}$	2932		2927					
	2872	2872	2871	2871	2871	2868	2872	2870
$\nu_{CH_2,\,as}$	2921	2930	2920	2928	2923	2926	2919	2925
$\nu_{CH_2,\,s}$	2861	2861	2856, 2852	2859	2851	2856	2850	2855
$\nu_{COO,\,as}$	1588	1585	1588	1586	1588	1585	1588	1585
		1542, 1532		1540, 1532		1541, 1530		1542, 1530
$\delta_{CH_3,\,as}$	1468, 1454	1458	1466, 1456	1456	1472, 1467	1454	1468, 1461	1456
$\delta_{CH_3,\,as}$	1445	1443	1448	1444	1447	1444	1449	1444
$\nu_{COO,\,s}$	1416	1423	1416	1424	1416	1425	1416	1425
		1416		1417		1417		1416
$\delta_{C_\alpha H_2}$	1407		1407		1404		1405	
δ_{CH_2}	1433	1443	1434	1444	1436	1444	1434	1444
$\delta_{CH_3,\,s}$	1378, 1367	1379, 1367	1379, 1369	1379, 1368	1378, 1363	1378, 1369	1379, 1354	1379, 1368
$\omega_{C_\alpha H_2}$	1345	1344	1357	1355	1342	1355	1326	1354
ω_{CH_2}	1313	1319	1323	1319	1314	1317	1311	1316
	1294	1305	1306	1312	1307	1279	1289	
$tw_{C_\alpha H_2}$	1279	1280	1273	1268	1260	1258	1276	1279
tw_{CH_2}	1230, 1212	1229, 1210	1250, 1221	1253, 1221	1242, 1214	1240, 1215	1249, 1209	1247, 1228
	1192	1189	1201, 1185	1202, 1179	1194, 1181	1196, 1173	1189, 1178	1190, 1169
ν_{C-C_α}	1111	1111	1118, 1111	1111	1114	1112	1115	1114
γ_{CH_3}	1060, 1054	1067	1083, 1051	1076, 1051	1068, 1064	1082, 1059	1071, 1061	1052
γ_{CH_3}	1035, 1010	1014	1036	1025, 1012	1044, 1031	1032, 1010	1042, 1010	1043, 1022
ν_{C-C}	988, 959	982, 962	982, 964	986, 961	990, 965	960	987	955
	921	912	941	945	941	927	941	947
$\nu_{C_\alpha-C(=O)}$	892, 847	890, 848	889, 841	889, 842	892, 878	896, 873	891, 878	893, 871
$\gamma_{C_\alpha H_2}$	805	803	818	821	832	834	831	827
γ_{CH_2}	792, 764	777	798, 771	773	800, 771	797, 760	797, 777	778
	746, 725	736	744, 723	727	755, 723	724	752, 722	723
δ_{COO}	668	686	668	685	668	686	668	686
		664		665		667		666
γ_{COO}	625, 594	624, 570	627, 589	624, 573	587	625	601, 587	624, 577
ω_{COO}	540, 494	521, 490	536, 509	518	537		486	509
	475	470	472	470	485	482	476	480
δ_{CCC}	452, 433	452, 435	451, 429	451	458, 424		455, 449	448, 432
	400		408		417		400	

Table 2—*Continued*

	wavenumber/cm^{-1}									
	CuC_{10}		CuC_{12}		CuC_{14}		CuC_{16}		CuC_{18}	
assignment	crystal	mesophase	crystal	mesophase	crystal	mesophase	crystal	mesophase	crystal	mesophase
$\nu_{CH_3,as}$	2955	2957	2955	2959	2955	2956	2955	2952	2956	2953
$\nu_{CH_3,as}$	2955	2957	2955	2959	2955	2956	2955	2952	2956	2953
$\nu_{CH_3,s}$	2931		2929		2929		2930		2930	
	2872	2868	2872	2870	2872	2870	2872	2870	2872	2870
$\nu_{CH_2,as}$	2942, 2917	2925	2941, 2916	2924	2942, 2915	2924	2942, 2915	2925	2941, 2915	2924
$\nu_{CH_2,s}$	2858, 2849	2855	2857, 2849	2854	2857, 2849	2854	2858, 2849	2854	2849	2854
$\nu_{COO,as}$	1585	1586	1586	1585	1586	1586	1586	1586	1586	1586
	1540, 1533		1542, 1533		1542, 1530		1542, 1528		1545, 153	
$\delta_{CH_3,as}$	1468	1457	1468	1458	1468	1458	1468	1456	1468	1458
$\delta_{CH_3,as}$	1446	1445	1447	1443	1446	1441	1445	1436	1446	1436
$\nu_{COO,s}$	1423	1425	1423	1424	1423	1424	1423	1425	1422	1425
	1417		1416		1417		1417		1418	
$\delta_{C_aH_2}$	1407		1407		1407		1407		1406	
δ_{CH_2}	1441, 1436	1445	1440	1443	1441	1441	1441	1436	1441	1436
$\delta_{CH_3,s}$	1377, 1364	1379, 1364	1378, 1368	1378, 1365	1378	1377, 1366	1378	1379, 1367	1380	1379, 1366
$\omega_{C_aH_2}$	1341	1342	1339	1356	1339	1351	1337	1354	1347	1355
ω_{CH_2}	1316	1317	1317	1317	1318	1319	1319	1317	1315	1317
	1303		1309, 1289		1312, 1295		1315, 1303		1302	
$tw_{C_aH_2}$	1276	1269	1258	1275	1270	1266	1279	1272	1266	1269
	1241, 1226	1240	1243, 1229	1250, 1223	1245, 1228	1243	1257, 1235	1246	1248, 1228	1244
tw_{CH_2}	1205, 1183	1208, 1166	1199, 1181	1198, 1165	1194, 1180	1187, 1163	1214, 1179	1169	1210, 1179	1170
	1118	1118	1118	1116	1118	1116	1118	1117	1118	1118
ν_{C-C_a}	1074, 1065	1079, 1056	1085, 1065	1071, 1042	1082, 1063	1079, 1066	1064	1089, 1072	1067	1094, 1072
γ_{CH_3}	1032, 1015	1034, 1006	1050, 1024	1035, 1008	1037, 1024	1030, 1008	1038, 1013	1031, 1005	1041, 1027	1031, 1022
γ_{CH_3}	994, 955	989, 961	981, 943	949	989, 949	955	978, 944	986	963	960
ν_{C-C}	943	930	930	933	942		931	944	943	
	890, 878	888, 877	892, 876	890, 876	891, 876	886	890, 877	889, 877	899, 872	889, 880
$\nu_{C_a-C(=O)}$	825	837	820	838	816	831	813	842	807	840
$\gamma_{C_aH_2}$	795, 776	764	794, 778	770	762, 754	769	782, 758	763	782, 761	764
γ_{CH_2}	743, 722	732, 720	733, 721	721	737, 721	721	741, 721	720	734, 721	721
	683	683	682	683	682	682	682	682	682	682
δ_{COO}		665		666		665		667		668
	624, 597	582	625, 597	622, 587	627, 588	619, 571	627, 588	621, 577	627, 598	621, 576
γ_{COO}	495	515	503	515	503	511	514	526	515	530
ω_{COO}			482				465	499	483	480
	439, 421		448, 438		457, 432		439, 427		440, 430	
δ_{CCC}	408		404		408		403		415	

[a] Crystal data obtained at room temperature; data in the mesophase obtained at *ca.* 150 °C.

Table 3 $\Delta\nu_{COO}(\nu_{COO,as} - \nu_{COO,s})$ and I_{2920}/I_{2850} for copper carboxylates[a]

	$\Delta\nu_{COO}$		I_{2920}/I_{2850}			
				mesophase		
compound	crystal	mesophase[b]	crystal[c]	$T \approx 125$	$T \approx 135$	$T \approx 150$
CuC_6	172	121	1.67	1.25	1.30	1.30
CuC_7	172	119	1.54	1.64	1.67	1.75
CuC_8	172	119	1.54	1.27	1.30	1.32
CuC_9	172	120	1.28	1.48	1.52	1.54
CuC_{10}	162	119	1.43	1.45	1.57	1.68
CuC_{12}	163	121	1.04	1.14	1.17	1.30
CuC_{14}	163	119	1.15	1.24	1.35	1.73
CuC_{16}	163	118	1.05	1.06	1.09	1.63
CuC_{18}	164	120	1.12	1.24	1.37	1.47

[a] Wavenumbers in cm^{-1}; temperatures in °C. [b] In the mesophase, those molecules exhibiting a chelating type coordination give rise to a doublet ascribable to $\nu_{COO,as}$ (see text) and, thus, $\Delta\nu_{COO}$ values were calculated using the average frequency for this mode and that of the lower component of the pair of bands due to the $\nu_{COO,s}$ mode. [c] Note that the compounds having shorter carbon chains present values for I_{2920}/I_{2850} in the crystal and in the mesophase which do not obey the general trend found for all the remaining molecules (though they follow the general pattern in the mesophase at different temperatures). This is certainly connected with the greater importance of the interactions involving the headgroups in these compounds.

result is in consonance with the absence of such kind of mesophases for the smaller members of the copper(II) carboxylates family (CuC_1–CuC_4[12]) and also agrees with data obtained by different methods (*e.g.* X-ray diffraction[11,12]).

On the other hand, the changes, associated with the phase transition, observed in the intensities and frequencies of the bands due to the ν_{COO} stretching modes, in particular the appearance of new bands, cannot be explained by taking into consideration only the above-mentioned increase in the carbon-chain conformational disorder. Though conformational disorder may indirectly provide the driving force leading to the structural modifications responsible for these changes, the observed spectral modifications must be due to an alteration of the coordination type. Thus, the bands near 1540 and 1417 cm^{-1} may be ascribed, respectively, to the $\nu_{COO,as}$ and $\nu_{COO,s}$ vibrations of those molecules exhibiting a

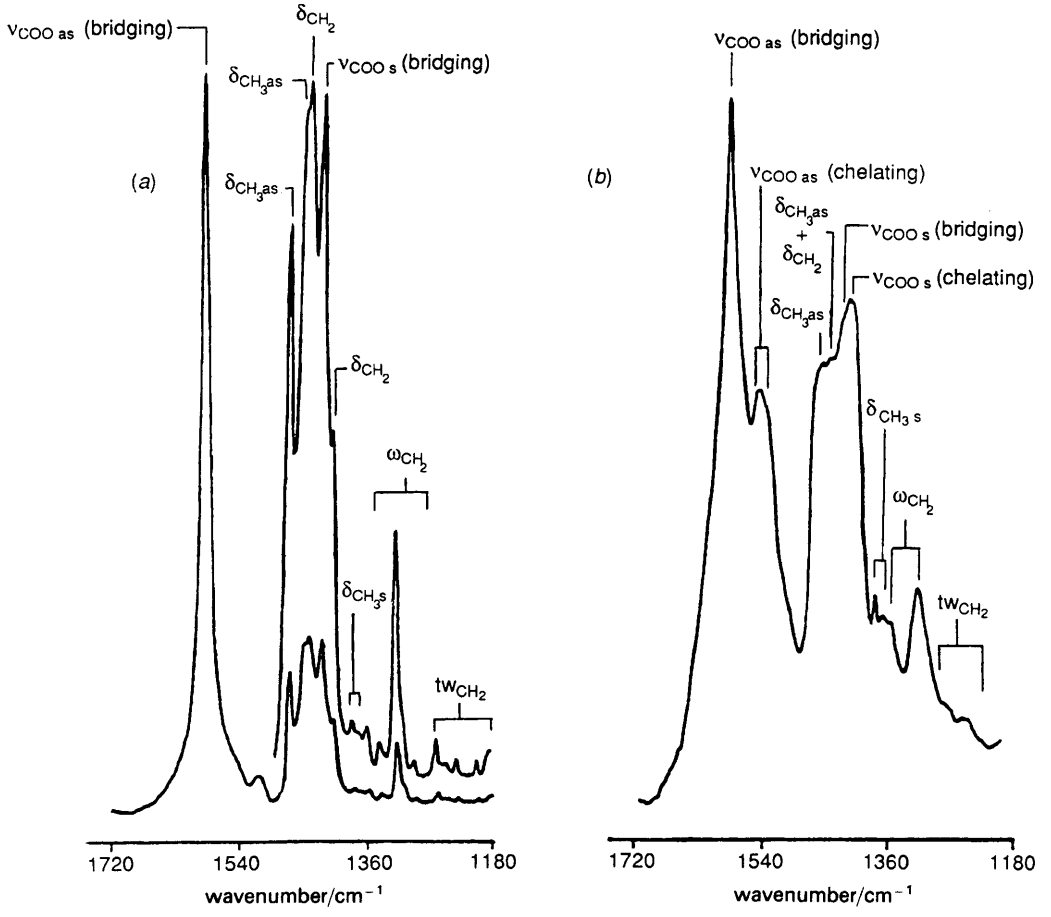

Fig. 4 Typical FTIR spectra profile of the copper(II) carboxylates, in the 1600–1400 cm^{-1} region, showing relevant band assignments: (*a*) crystal (room temperature); (*b*) columnar mesophase ($T \approx 150$ °C)

different type of coordination from the bridging bidentate structure found in the crystals. In particular, considering the $\Delta\nu_{COO}$ values associated with these new bands (*ca.* 120 cm^{-1}; see Table 3) it can be proposed that the new type of coordination should correspond to the chelating bidentate structure (structure II, Fig. 3), which is also found, for example, in zinc and cadmium long-chain carboxylates at room temperature.[20] Note that the proposed global arrangement of the chelating bidentate carboxylates around the copper atoms (Fig. 5) is consistent with the data previously obtained by EXAFS,[3,14] which allowed to conclude that, though a structural modification around the binuclear copper core occurs at the phase transition, the number of oxygen atoms around each copper atom is the same, the Cu—O bond lengths do not change appreciably and only a very slight increase in the Cu—Cu bond length seems to occur. In addition, besides being geometrically possible, the bridging bidentate → chelating bidentate modification is also possible in mechanistic terms. In fact, the chelating bidentate structure may be obtained from the bridging bidentate structure by means of a *ca.* 90° concerted rotation of the four carboxylate groups, implying only minor changes in both the O—C—O and O—Cu—O angles (which have to increase and decrease slightly, respectively) and a small lengthening of the C—O bonds (Fig. 5).

Note that the geometrically required changes in the O—C—O and O—Cu—O angles discussed above are also in consonance with the EXAFS studies,[3,14] from which it was concluded that the structural changes associated with the phase transition should involve mainly angular distortions.

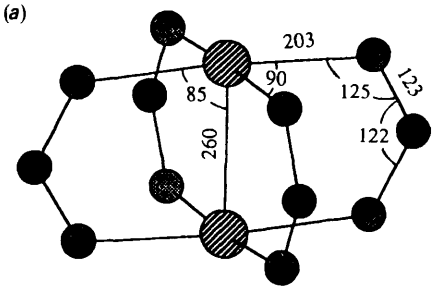

bridging bidentate coordination

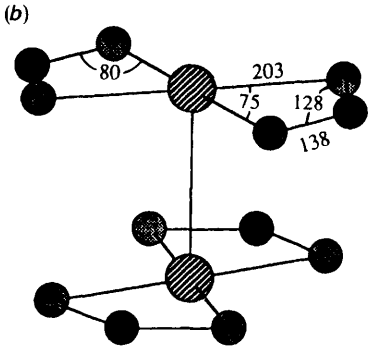

chelating bidentate coordination

Fig. 5 Carboxylate–metal coordination structures of copper (II) carboxylates in (*a*) the crystalline (bridging bidentate coordination) and (*b*) the columnar liquid-crystalline (chelating bidentate coordination). The indicated geometric parameters (in units of pm or degrees) for the crystal were typical values taken from available X-ray or EXAFS data;[3,8–10,14] those presented for the mesophase were obtained in this study by molecular modelling.

In turn, the required lengthening of the C—O bonds agrees with the observed frequency red shift found for the ν_{COO} stretching modes (in particular for $\nu_{COO,as}$) which gives rise to new bands. It is also interesting to note that the slight lengthening of the Cu—Cu distance, observed by EXAFS, upon phase transition[3,14] is also consistent with the proposed change in the type of coordination, as the presence of the bridging carboxylates in the crystal certainly tends to force the copper atoms to approach each other.

Finally, the simultaneous presence of the two types of coordinating structures (bridging and chelating) in the mesophase can also be inferred from the IR spectroscopic results, since, besides the new ν_{COO} bands due to the chelating carboxylates, the ν_{COO} bands assigned to bridging carboxylates also appear in the IR spectra of the mesophase at frequencies similar to those found in the crystal (this is particularly evident for $\nu_{COO,as}$, owing to the higher intensity of the bands ascribed to this mode, see Fig. 4). In the mesophase, the relative intensities of the bands ascribed to the chelating (*ca.* 1540 cm^{-1}) and bridging (*ca.* 1585 cm^{-1}) carboxylates (I_{1540}/I_{1585}) do not change appreciably with temperature. However, for the longer-chain carboxylates studied (CuC_{12}–CuC_{18}) the I_{1540}/I_{1585} intensity ratio decreases slightly with increasing temperature. While the increase in the conformational disorder that occurs upon raising the temperature (Table 3) can, in principle, be directly responsible for the observed changes in I_{1540}/I_{1585}, these changes are most probably due to an effective change in the relative population of the two types of coordination, the bridging structure having an increase in relative population with temperature. Thus, considering that in the mesophase an equilibrium exists between the two types of coordination, the results point to a bridging structure with a higher energy in this phase than the chelating coordination, as might be expected. However, the energy difference between the two types of coordination appears to decrease when the carbon chain becomes smaller, as no significant changes were observed in I_{1540}/I_{1585} for the smaller compounds studied. Thus, these results reinforce our previous conclusion that carbon-chain conformational disordering plays a very important role in determining the structural changes, including the change in the coordination type, occurring at the phase transition. In addition, they are also consistent with the observed correlation between the carbon-chain size of the carboxylates and the crystal-to-mesophase transition temperatures.[12]

800–600 cm^{-1} Region

In this spectral region, the most prominent bands are due to the γ_{CH_2} rocking (*ca.* 720 cm^{-1}) and δ_{COO} scissoring modes. In the crystalline state, the scissoring mode gives rise to a single band, which appears at *ca.* 685 cm^{-1} for the longer-chain compounds and at *ca.* 669 cm^{-1} for the smaller compounds (CuC_6–CuC_9). In the mesophase, the band ascribed to the γ_{CH_2} rocking broadens, and a pair of bands of nearly equal intensities are ascribed to the δ_{COO} scissoring vibration (Fig. 6).

The observed broadening may be ascribed, at least in part, to the increase in the conformational disorder in the carbon chains, while the splitting of the band ascribed to the δ_{COO} scissoring mode is most probably due to the change in the type of coordination associated with the phase transition. The higher-frequency component of the doublet due to the δ_{COO} scissoring vibration is ascribed to the bridging carboxylates, while the lower-frequency component is assigned to the chelating carboxylates. In fact, it was shown previously[13] that a red shift in the frequency of the δ_{COO} scissoring mode is expected when the O—C—O angle increases (this may be

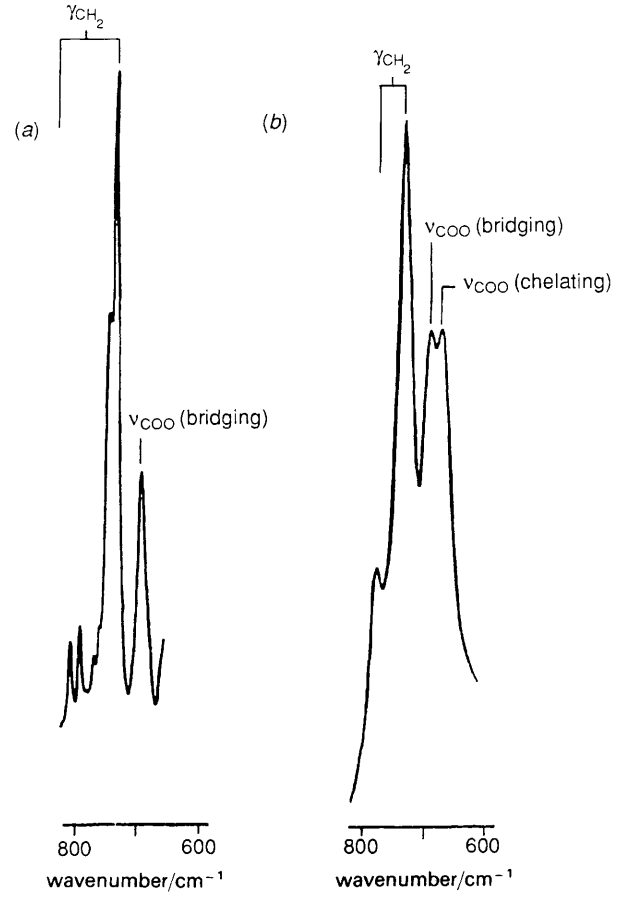

Fig. 6 Typical FTIR spectra profile of the studied copper(II) carboxylates, in the 800–600 cm^{-1} region, showing relevant band assignments: (*a*) crystal (room temperature), (*b*) columnar mesophase ($T \approx 150$ °C)

easily understood if one considers that if the angle is forced to assume a value larger than in its non-stressed equilibrium geometry then the effective force constant associated with the δ_{COO} scissoring mode must decrease). Thus, remembering that, as mentioned above, the bridging → chelating change in coordination requires an opening of the O—C—O angles, the proposed assignments may be easily justified and further reinforce the conclusions obtained by analysis of the ν_{COO} stretching spectral region.

Conclusion

IR spectroscopy has been shown to be a suitable method for following thermotropic phase transitions in copper(II) carboxylates and, in particular, has provided the key to the understanding of the structural reorganization processes that are associated with the crystalline → columnar liquid-crystalline-phase transition. Above the transition temperature, the spectra show notable changes associated with both the increase in the conformational disorder of the carbon chains and the change in the coordination of the carboxylate groups to the bimetallic centre from bridging bidentate to chelating bidenate type. The data available on the studied componds (including that previously obtained[11] for the smaller molecules of the series, CuC_1–CuC_4, which do not present the columnar mesophase) indicate that the change in the type of coordination is most probably induced by the conformation disorder in the carbon chains. The proposed global arrangement of the chelating bidentate carboxylates around the copper atoms is both geometrically and mechanistically consistent with the data previously obtained by EXAFS.[3,14]

The authors thank Profs. H.D. Burrows (Department of Chemistry, University of Coimbra), M.O. Figueiredo (Centro de Cristalografia e Mineralogia, I.I.C.T., Lisbon) and A.C Fernandes (Centro de Química Estrutural, Instituto Superior Técnico, Lisbon), for making available the equipment used to carry out the optical microscopy, X-ray powder diffraction and differential scanning calorimentry studies, respectively. M.F.R.M. acknowledges financial support from Junta Nacional de Investigacão Científica e Tecnológica (J.N.I.C.T.), Portugal (Grant n BD/1239/91/RM).

References

1 F. A. Cotton, *Acc. Chem. Res.*, 1978, **11**, 225.
2 Y. B. Koh and G. G. Christoph, *Inorg. Chem.*, 1979, **18**, 1122.
3 P. Maldivi, D. Guillon, A. M. Giroud-Godquin, J. C. Marchon, H. Abied, H. Dexpert and A. Skoulios, *J. Chim. Phys.*, 1989, **86**, 1651.
4 H. Abied, D. Guillon, Al Skoulios, H. Dexpert, A. M. Giroud-Godquin and J. C. Marchon, *J. Phys. Fr.*, 1988, **49**, 345.
5 F. J. Buono and M. L. Feldman, in *Kirk-Othmer Encyclopedia of Chemical Technology*, ed. A. F. Mark, D. F. Othmer, C. G. Overberger and G. T. Seaborg, Wiley, New York, 3rd edn., 1979, vol. 8, p.34.
6 A. S. Lindsey, H. D'Souza, F. A. Rackley, G. H. Risebrow-Smith and H. R. Whitehead, *NPL Report Chem.*, 1978, **87**, 1.
7 M. S. Akanni, E. K. Okoh, H. D. Borrows and H. A. Ellis, *Thermochim. Acta*, 1992, **208**, 1.
8 M. J. Bird and T. R. Lomer, *Acta Crystallogr., Sect. B*, 1972, **28**, 242.
9 T. R. Lomer and K. Perera, *Acta Crystallogr., Sect. B*, 1974, **30**, 2912.
10 T. R. Lomer and K. Perera, *Acta Crystallogr., Sect. B*, 1974, **30**, 2913.
11 H. Abied, D. Guillon, A. Skoulios, P. Weber, A. M. Giroud-Godquin and J. C. Marchon, *Liq. Cryst.*, 1987, **2**, 269.
12 M. Ibn-Elhaj, D. Guillon, A. Sloulios, A. M. Giroud-Godquin and P. Maldivi, *Liq. Cryst.*, 1992, **11**, 731.
13 R. Fausto and J. J. C. Teixeira-Dias, *Pure Appl. Chem.*, 1989, **61**, 959.
14 J. C. Marchon, P. Maldivi, A. M. Giroud-Godquin, D. Guillon, A. Skoulios and D. P. Strommen, *Philos. Trans. R. Soc. London.*, 1990, **330**, 109.
15 A. M. Giroud-Godquin, J. N. Latour and J. C. Marchon, *Inorg. Chem.*, 1985, **24**, 4452.
16 D. P. Strommen, A. M. Giroud-Godquin, P. Maldivi and J. C. Marchon, *Liq. Crys.*, 1987, **2**, 689.
17 R. Wargo, D. MacFerren, J. A. Sterling, K. Mishra and A. L. Smith, *MOLECULAR EDITOR* (*Version 1.1*), Department of Chemistry, University of Drexel, USA, 1987.
18 M. F. Ramos Moita, M.L.T.S. Duarte and R. Fausto, to be published.
19 Y. Mathey, D. R. Greig and D. F. Shriver, *Inorg. Chem.*, 1982, **21**, 3409.
20 M. A. Mesubi, *J. Mol. Struct.*, 1982, **81**, 61.
21 N. Nakamoto and P. J. McCarthy, *Spectroscopy and Structure of Metal Chelate Compounds*, Wiley, New York, 1968, p. 268.
22 D. A. Edwards and R. N. Hayward, *Can. J. Chem.*, 1968, **46**, 3643.
23 E. V. van der Berghe, G. P. van der Kelen and J. Albrecht, *Inorg. Chim. Acta*, 1968, **2**, 89.
24 N. W. Alcock, V. M. Tracy and T. C. Waddington, *J. Chem. Soc., Dalton Trans.*, 1976, 2243.
25 R. A. Meiklejohn, R. J. Mayer, S. M. Aronovic and H. A. Schuette, *Anal Chem.*, 1957, **29**, 329.
26 J. B. Rosenholm, P. Stenius and I. Danielsson, *J. Colloid Interface Sci.*, 1976, **57**, 551.
27 K. Larsson and R. P. Rand, *Biochim. Biophys. Acta*, 1973, **326**, 245.
28 I. R. Hill and I. W. Levin, *J. Chem. Phys.*, 1979, **70**, 842.

Paper 4/02795G; *Received* 11*th May*, 1994